

Simultaneous Phase- and Size-Controlled Synthesis of TiO₂ Nanorods via Non-Hydrolytic Sol–Gel Reaction of Syringe Pump Delivered Precursors

Bonil Koo,[†] Jongnam Park,[†] Yukyeong Kim,[‡] Sang-Hyun Choi,[†] Yung-Eun Sung,[‡] and Taegwan Hyeon^{*,†}

National Creative Research Center for Oxide Nanocrystalline Materials and School of Chemical and Biological Engineering, Seoul National University, Seoul 151-744, Korea, and School of Chemical and Biological Engineering, Seoul National University, Seoul 151-744, Korea

Received: August 18, 2006; In Final Form: September 29, 2006

The simultaneous phase- and size-controlled synthesis of TiO₂ nanorods was achieved via the non-hydrolytic sol–gel reaction of continuously delivered two titanium precursors using two separate syringe pumps. As the injection rate was decreased, the length of the TiO₂ nanorods was increased and their crystalline phase was simultaneously transformed from anatase to rutile. When the reaction was performed by injecting titanium precursors contained in two separate syringes into a hot oleylamine surfactant solution with an injection rate of 30 mL/h, anatase TiO₂ nanorods with dimensions of 6 nm (thickness) × 50 nm (length) were produced. When the injection rate was decreased to 2.5 mL/h, star-shaped rutile TiO₂ nanorods with dimensions of 25 nm × 200 nm and a small fraction of rod-shaped anatase TiO₂ nanorods with dimensions of 9 nm × 100 nm were synthesized. Pure star-shaped rutile TiO₂ nanorods with dimensions of 25 nm × 450 nm were synthesized when the injection rate was further decreased to 1.25 mL/h. The simultaneous phase transformation and length elongation of the TiO₂ nanorods were achieved. Under optimized reaction conditions, as much as 3.5 g of TiO₂ nanorods were produced. The TiO₂ nanorods were used to produce dye-sensitized solar cells, and the photoconversion efficiency of the mixture composed of star-shaped rutile TiO₂ nanorods and a small fraction of anatase nanorods were comparable to that of Degussa P-25.

Introduction

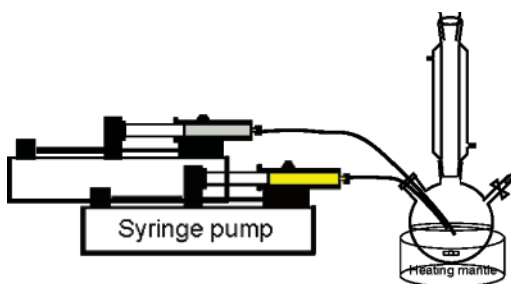
Recently, one-dimensional (1-D) nanostructured materials including nanorods and nanowires have been intensively studied because of their unique electrical,¹ magnetic,² and optical³ properties, which are derived from their low dimensionality and quantum size effect, and because of their many potential technological applications such as interconnects and functional building blocks for nanodevices.⁴ For the past decade, nanorods and nanowires of magnetic materials,⁵ noble metals,⁶ and semiconductors⁷ have been synthesized using various methods. Titania (TiO₂) is an n-type wide band-gap semiconductor material with a band gap energy of 3.2 eV and has been used in a wide variety of applications, including dye-sensitized solar cells (DSSC),⁸ photocatalysts,⁹ and photochromic devices.¹⁰ 1-D TiO₂ nanocrystals have several advantages over their spherical counterparts in terms of their potential applications because of their high surface-to-volume ratio, increased number of delocalized carriers, and improved charge transport afforded by their dimensional anisotropy, as reported by Cozzoli et al.¹¹ Recently, several different synthetic routes have been employed to produce 1-D TiO₂ nanocrystals. These include hydrothermal synthesis,¹² the sol–gel process,¹³ surfactant-mediated synthesis,^{11,14} and template synthesis.¹⁵ Chemseddine and Moritz reported the synthesis of uniform-sized TiO₂ nanocrystals with various shapes depending on the ratio of Me₄NOH to titanium alkoxide.^{13a} However, the concentration of the reactants was very low in

this synthesis, resulting in the products being obtained in low yields. Cozzoli et al. reported the controlled growth of TiO₂ nanocrystals using the modulation of the hydrolysis rate in the presence of oleic acid as a surfactant at 80 °C.¹¹ Jun et al. and Seo et al. reported the surfactant-mediated shape evolution of TiO₂ nanorods in nonaqueous media.^{14a,b} Adachi et al. synthesized anatase nanowires via the controlled hydrolysis of titanium(IV) isopropoxide accompanied by the use of an oriented attachment mechanism for dye-sensitized solar cells.^{14b} Various nonhydrolytic sol–gel reactions have been used to synthesize nanocrystals of many transition-metal oxides.¹⁶ Trentler et al. synthesized TiO₂ nanocrystals via a nonhydrolytic alkyl halide elimination reaction.^{16c} Our research group employed a similar procedure to produce ZrO₂ nanocrystals,^{16f} and Tang et al. further extended these synthetic methods to produce nanocrystals of HfO₂ and Hf_xZr_{1-x}O₂.^{16g} Very recently, our group synthesized nanocrystals of TiO₂ and ZnO via non-hydrolytic ester elimination reactions.¹⁷ Recently, our research group developed a new synthetic route to produce uniform-sized nanorods and nanowires via the thermal decomposition of syringe pump delivered precursors in hot surfactant solution.¹⁸ By combining the non-hydrolytic sol–gel reaction and the thermal decomposition of the syringe pump delivered precursors, we were able to synthesize uniform-sized TiO₂ nanorods while simultaneously varying their phase and size. Because Degussa P-25 TiO₂, which is composed of anatase and rutile phases at a ratio of ca. 80:20, is known to be one of the most active photocatalysts owing to the synergic effect of the two components,¹⁹ we investigated the photocatalytic activities of the currently synthesized TiO₂ nanorods with various ratios of phases and sizes.

* Author to whom correspondence should be addressed. E-mail: thyeon@snu.ac.kr.

[†] National Creative Research Center for Oxide Nanocrystalline Materials and School of Chemical and Biological Engineering.

[‡] School of Chemical and Biological Engineering.

SCHEME 1: Schematic Illustration of the Experimental Setup for the Synthesis of TiO₂ Nanorods**Experimental Section**

Chemicals. Hexane, cyclohexane, ethanol, acetone, and water were distilled and degassed before use. Titanium(IV) chloride (TiCl₄, 99.9%), titanium(IV) isopropoxide (TTIP, 97%), 1-octadecene (90%), and oleic acid (99+%) were purchased from Aldrich Chemicals. Oleylamine was purchased from TCI. Oleylamine, 1-octadecene, and oleic acid were purified by vacuum distillation before use.

Synthesis of TiO₂ Nanorods. In our synthesis, we used syringe pumps to enable the continuous supply of the titanium precursor solutions into the hot surfactant solution. In a typical synthesis, two separate titanium precursor solutions were prepared by mixing 0.22 mL of TiCl₄ and 4.78 mL of 1-octadecene and similarly mixing 0.59 mL of TTIP and 4.41 mL of 1-octadecene at room temperature. The two 5 mL of titanium precursor solutions contained in two separate syringe pumps were continuously injected into 2 mL of oleylamine under vigorous stirring at 300 °C via a syringe pump with various injection rates of 30 mL/h, 2.5 mL/h, and 1.25 mL/h, which correspond to total reaction times of 10 min, 2 h, and 4 h, respectively. Smoke evolved quite intensely and the color of the solution changed from dark purple to yellow during the reaction, indicating that TiO₂ nanorods were formed by the non-hydrolytic sol-gel reaction. By adding 50 mL anhydrous acetone to the resulting solution, the flocculation of the TiO₂ nanorods was brought about. After centrifugation, the flocculated nanorods were isolated from the supernatant and were washed two or three times with 50 mL acetone to remove the excess

oleylamine or 1-octadecene. The final precipitate was vacuum-dried and obtained in the form of an off-white powder. The TiO₂ nanorod powders made using these procedures were readily dispersed in organic solvents such as hexane or cyclohexane. For the large-scale synthesis, the amount of the reagents, including titanium precursors, 1-octadecene, and oleylamine, was increased to 10 times of that used above.

Preparation for Dye-Sensitized Solar Cells (DSSC). For the preparation of dye-sensitized solar cells (DSSC), three viscous suspensions of TiO₂ (anatase, rutile, and anatase 81% + rutile 19%) powders were prepared by adding them to an ethanol solution of TritonX-100 surfactant (from Aldrich). These suspensions were deposited on an F-doped conducting glass substrate (Solaronix SA, 10 Ω/M) by the doctor blade coating method with a glass and scotch tape as a frame and spacer, respectively. The deposited TiO₂ film was sintered at 450 °C for 1 h under air.

The photoelectrodes prepared using the various TiO₂ powders were immersed in an absolute ethanol solution of 0.5 mM Ru 535 dye (Solaronix Co. Ltd.). Counter electrodes were prepared by the sputtering of Pt on ITO glass and the electrolyte was composed of 0.5 M LiI, 0.05 M I₂, and 0.5 M *tert*-butyl pyridine in methoxypropionitrile. Using these components, a sandwich type configuration was fabricated, and this was employed to measure the performance of the cell. The active area of the cells was adjusted to 0.25 cm². The film thickness and surface morphology of the deposited film was observed using scanning electron microscopy (SEM). The cell performance was measured using a solar simulator (Seric) with intensity of 100 mW/cm² through an AM 1.5 filter. Photocurrent-voltage (*I*-*V*) measurements were performed using an Autolab PGSTAT30 potentiostat/galvanostat.

Material Characterization. The titania nanorods were characterized by low- and high-resolution transmission electron microscopy (TEM), electron diffraction (ED), and X-ray diffraction (XRD). The TEM images were collected on a JEOL JEM-2010 electron microscope operating at 200 kV. The XRD patterns were obtained using a Rigaku D/Max-3C diffractometer equipped with a rotation anode and a Cu Kα radiation source ($\lambda = 0.15418$ nm). The elemental analysis of the TiO₂ nanorods was conducted by X-ray photoelectron spectroscopy (XPS) using

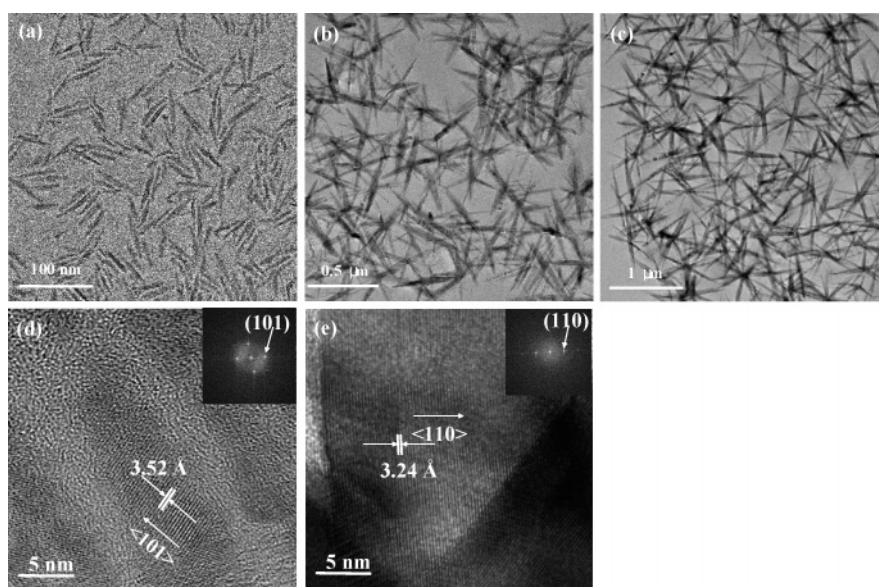


Figure 1. TEM images of TiO₂ nanorods obtained using an injection rate of (a) 30 mL/h, (b) 2.5 mL/h, and (c) 1.25 mL/h, respectively. High-resolution TEM images of Figure a and (e) rutile of Figure c.

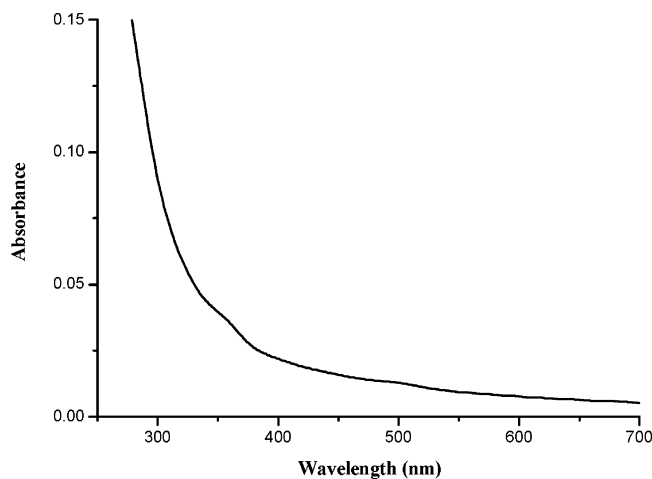


Figure 2. UV-vis absorption spectrum of anatase TiO₂ nanorods with dimensions of 6 nm × 50 nm.

a Sigma Probe (Thermo VG, United Kingdom) electron spectroscope for the chemical analysis (ESCA) and an Al anode as a monochromatic X-ray source. The optical properties of the TiO₂ nanorods were characterized by means of a Perkin-Elmer Lambda Model 20 UV-vis spectrometer.

Results and Discussion

Synthesis of Size- and Phase-Controlled TiO₂ Nanorods.

The titania nanorods were synthesized by the non-hydrolytic sol-gel reaction of syringe pump delivered precursors.¹⁸ The subsequent non-hydrolytic alkyl halide elimination reaction was employed for the synthesis of the TiO₂ nanorods (eq 1).^{16c}



Two syringe pumps were used to provide the continuous and constant delivery of two titanium precursor solutions, thus inducing a continuous reaction and one-dimensional growth of uniform-sized nanoparticles. Scheme 1 represents a schematic

illustration of the experimental setup employed for the synthesis of TiO₂ nanorods using syringe pumps. By varying the injection rates, we were able to simultaneously control the crystalline phase and size of the nanorods. Furthermore, the morphology of the TiO₂ nanorods evolved to a branched shape while their length was also increased.

Figure 1a shows the anatase TiO₂ nanorods with dimensions of 6 nm (diameter) × 50 nm (length), which were synthesized by delivering the titanium precursors at a syringe pump injection rate of 30 mL/h. Figure 1b shows the star-shaped rutile TiO₂ nanorods with dimensions of 25 nm × 200 nm mixed with a small amount of rod-shaped anatase TiO₂ nanorods with sizes of 9 nm × 100 nm, which were produced by the continuous injection of the precursors at a rate of 2.5 mL/h. Finally, Figure 1c shows only star-shaped rutile TiO₂ nanorods with dimensions of 25 nm × 450 nm, which were obtained using an injection rate of 1.25 mL/h.

Figure 1d and 1e shows the high-resolution transmission electron microscopic (HRTEM) images of the anatase nanorods with dimensions of 6 nm × 50 nm (TEM image in Figure 1a) and star-shaped rutile nanorods (TEM image in Figure 1c), respectively. The <101> lattice planes of the anatase structure were clearly observed in Figure 1d, while the <110> lattice planes of the rutile structure were evident in Figure 1e.

The UV-vis absorption spectrum of the anatase TiO₂ nanorods measured at room temperature exhibited typical absorption characteristics of TiO₂ nanoparticles (Figure 2). The peak maximum was calculated to be 340 nm, which is ~45 nm blue-shifted from that of bulk anatase. This 45-nm blue-shift seems to be resulted from the quantum size effect. The exciton radius of TiO₂ is known to be in the range of 7.5–1.9 nm.¹⁷

The length of the TiO₂ nanorods was inversely proportional to the injection rate of the titanium precursor solutions. This result demonstrates that titania seeds were formed in the early stage of the synthesis and that the subsequent addition and thermolysis of the precursors contributed to the growth of the nanorods. A similar tendency was observed for our previous synthesis of Fe₂P nanorods via the thermal decomposition of a

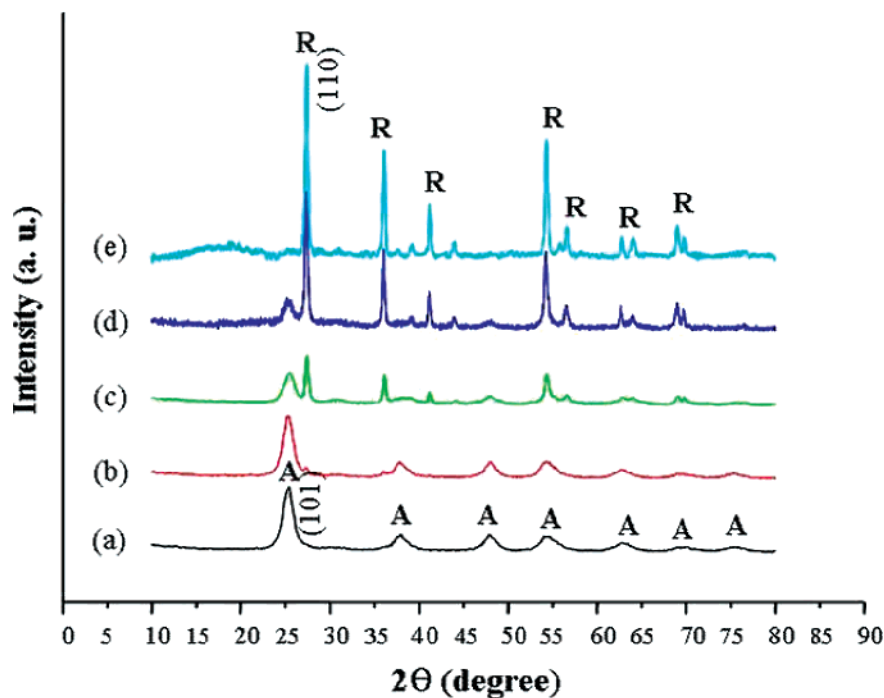


Figure 3. X-ray diffraction patterns of TiO₂ nanorods synthesized by a syringe pump: (a)–(e) injection rate = 30 mL/h, 20 mL/h, 5 mL/h, 2.5 mL/h, and 1.25 mL/h, respectively. R and A pointed above peaks denote rutile and anatase, respectively.

TABLE 1: Crystal Phase Ratios of TiO₂ Nanorods Synthesized at Various Injection Rates of Syringe Pump

injection rate	relative strongest XRD peak intensity		weight percentage	
	rutile (I_R)	anatase (I_A)	rutile	anatase
30 mL/h	0	100.0	0%	100%
20 mL/h	18.6	100.0	19%	81%
5 mL/h	100.0	64.2	66%	34%
2.5 mL/h	100.0	20.6	86%	14%
1.25 mL/h	100.0	0	100%	0%

syringe pump delivered Fe-TOP complex.^{18a} The syringe pump played a critical role in the growth step of the nanocrystals, thus controlling the length of the TiO₂ nanorods. When a single injection of titanium precursors was performed, without using a syringe pump, a mixture of polydispersed nanoparticles and short nanorods was produced (Supporting Information, SI), which was consistent with the previous report by Trentler et al.^{16c}

Phase Transformation of TiO₂ Nanorods. The crystalline phase of TiO₂ nanorods was simultaneously varied by changing the injection rate. At the fast injection rate of 30 mL/h, pure anatase nanorods were produced. As the injection rate decreased, the fraction of rutile phase increased. Finally, only rutile nanorods were produced at the slowest injection rate of 1.25 mL/h. As described above, the size of the nanorods also increased as the injection rate decreased. The crystal structures of the nanorods were characterized by HRTEM (Figure 1d and 1e) and X-ray diffraction (XRD) studies (Figure 3).

A quantitative analysis of crystal structure of the nanorods was performed using the following equation.²⁰

$$X_A = [1 + 1.26 (I_R/I_A)]^{-1} \quad (2)$$

where X_A indicates the weight fraction of anatase in the products, and I_R and I_A are the intensities of the strongest diffraction peak of rutile and anatase phase in the XRD patterns. Table 1 shows ratios of two crystal phases of the TiO₂ nanocrystals synthesized at various injection rates.

The composition of the crystal phases seems to be related to the dimensions of the nanorods.²¹ As described above, the larger sized nanorods consisted of rutile phase, whereas anatase phase was dominant for the smaller sized nanorods. This tendency was presumably because certain crystal structures are more stable than others in a given size regime, because of the surface free energy, as reported by Garvie.^{21a,21b} In the current synthesis, the diameter of the TiO₂ nanorods, rather than their length, was the determining factor in the phase transformation. The critical diameter for the phase transformation from anatase to rutile was approximately 15 nm. This result was very similar to the previous report by Zhang and Banfield on the phase stability of titania nanocrystals.^{21c}

The transformation from anatase phase to rutile phase from annealing at high temperature is well-known, and this transformation is known to be even more accelerated for nanocrystalline titania.²¹ The gradual transformation of anatase phase to rutile phase by decreasing the injection rate can be explained by the corresponding increase in the reaction time.

To obtain a better understanding of the phase transformation, we conducted a series of sampling experiments during the synthesis of the TiO₂ nanorods using a slow injection rate of 1.25 mL/h. Some of the TEM images of the aliquots of the reaction mixture taken every 10 min are shown in Figure 4.

The TEM and corresponding HRTEM images after allowing the reaction to proceed for 10 min revealed the presence of anatase nanorods with dimensions of 7 nm × 40 nm. After the reaction had proceeded for 20 min, thicker and branched 15 nm × 60 nm sized nanorods with a rutile crystal structure started to appear. This was consistent with the explanation that the critical diameter for the phase transformation was 15 nm. After the rutile phase appeared, the nanorods started to assemble to form V-shaped (bipod) or Y-shaped structures and then finally to produce star-shaped nanorod assemblies with predominant rutile phase. To the best of our knowledge, this is the first report of the synthesis of star-shaped TiO₂ nanorods.

Large-Scale Synthesis. The current synthetic procedure can be readily utilized for the large multigram scale production of the nanorods. For example, when 10 times larger amount of

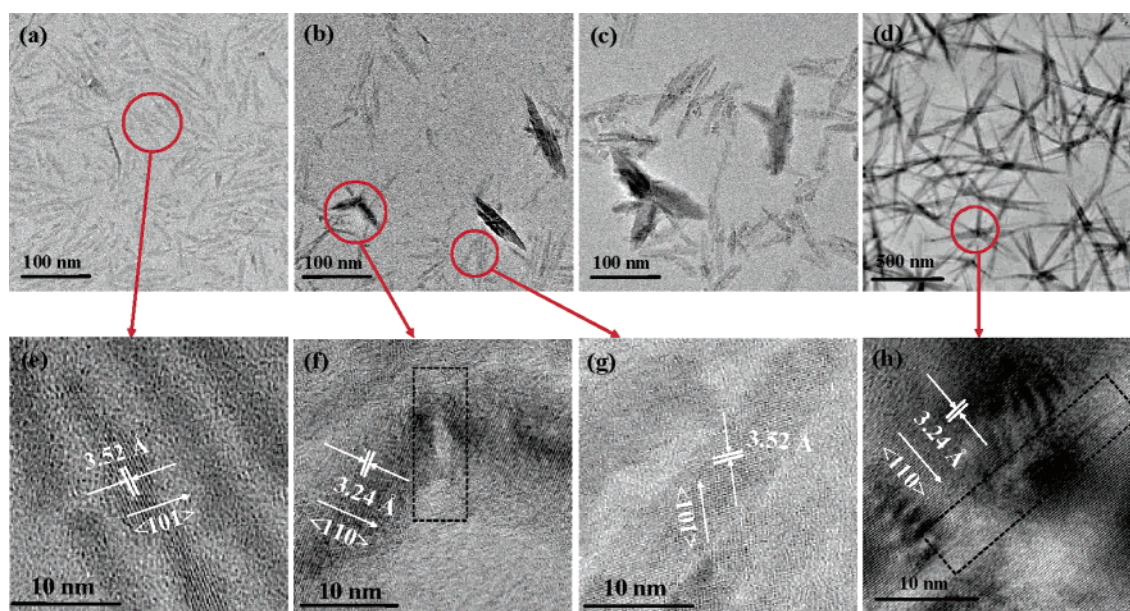


Figure 4. Normal TEM images of TiO₂ nanorods obtained at (a) 10 min, (b) 20 min, (c) 30 min, and (d) 4 h, respectively, after initial injection using an injection rate of 1.25 mL/h. High-resolution TEM images of (e) anatase nanorods of a, (f) rutile nanorods of b, (g) anatase nanorods of c, and (h) rutile nanorods of d. Particularly, f and h indicated the central area of bridged rutile nanorods, and dotted lines showed crystal defects of the center of each sample.

TABLE 2: Crystal Size, BET, Fill Factor (ff), Open-Circuit Photovoltage (V_{oc}), Short-Circuit Photocurrent (J_{sc}), and Conversion Efficiency (η) of the Samples^a

samples (phase, composition)	dimensions (nm)	BET (m ² /g)	FF (%)	V_{oc} (V)	J_{sc} (mA/cm ²)	η (%)
pure anatase nanorods	6 nm × 50 nm	131.18	53.5	-0.730	9.07	3.54
81% anatase and 19% rutile	5 nm × 60 nm(A) + 15 nm × 80 nm (R)	115.52	55.8	-0.740	9.27	3.83
pure star-shaped rutile nanorods	25 nm × 450 nm	2.07	61.2	-0.723	4.79	2.12

reagents compared to the original synthesis was used, we were able to synthesize as much as 3.5 g of the phase- and size-controlled TiO₂ nanorods. The success of scale-up method could be explained by the reason that the slow dropwise delivery of precursors via a syringe pump prevented a particle aggregation which usually hinders a large-scale synthesis. This result demonstrated that the synthetic procedure for the nanorods via the thermolysis of syringe pump delivered precursors could be applied to the large scale synthesis of well-controlled nanorods.

Application of Dye-Sensitized Solar Cells (DSSC). Figure 5 shows the I - V curves of the DSSCs fabricated using a conventional TiO₂/Ru 535 dye electrode. The DSSC fabricated using a 10- μ m-thick film coated with TiO₂ nanorods with an anatase-to-rutile ratio of 81:19 generated an open-circuit photovoltage (V_{oc}) of 740 mV, a short-circuit photocurrent (J_{sc}) of 9.27 mA/cm², a fill factor (ff) of 55.8%, and a conversion efficiency (η) of 3.83%. Table 2 summarizes the characteristics and DSSC performance of three nanocrystalline TiO₂ film electrodes.

As shown in Figure 5 and Table 2, the electrode fabricated using a mixture of anatase (81%) and rutile (19%) phases showed a conversion efficiency (η value) of 3.83%, which is comparable to that of a mesoporous TiO₂ electrode fabricated using commercial Degussa P-25 (4.10%).

For many applications such as dye-sensitized solar cells, TiO₂ nanoparticles are needed which are dispersible in aqueous media. There have been several previous reports on the transformation of nanoparticles synthesized in organic media into water-dispersible nanoparticles. Oftentimes, these processes are complicated and limited. Fortunately, however, we were able to remove the stabilizing surfactants from the TiO₂ nanorods simply by washing them with water. The typical procedure used for the water treatment is as follows. The synthesized TiO₂ nanorods were first washed with acetone, and the resulting powder was dispersed in water. The aqueous dispersion was sonicated for 5 min and white powdery nanorods were obtained by filtration. Subsequently, three cycles of washing with acetone and centrifugation generated water-dispersible TiO₂ nanorods.

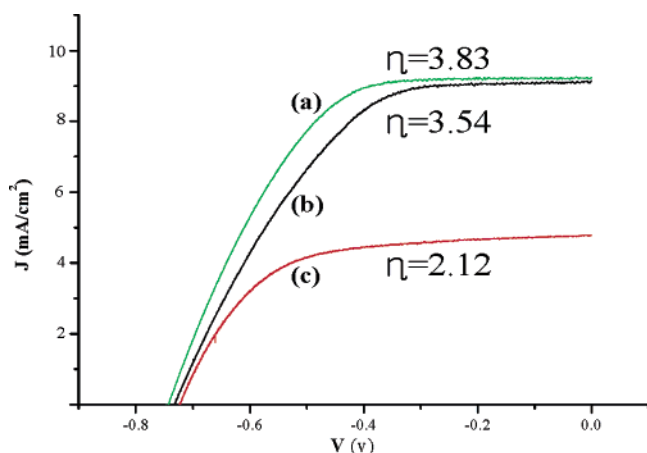


Figure 5. I - V curves of a DSSC fabricated by a conventional TiO₂/Ru 535 dye electrode using (a) a mixture of 81% anatase and 19% rutile, (b) pure anatase nanorods, and (c) star-shaped rutile nanorods.

The XPS analysis conducted after the washing process showed that oleylamine was completely removed from the TiO₂ nanorods (Supporting Information).

Conclusions

In summary, the simultaneous phase- and size-controlled synthesis of TiO₂ nanorods was achieved via the non-hydrolytic alkyl halide elimination reaction of titanium precursors continuously delivered via syringe pumps. The synthetic procedures are highly reproducible and offer several significant advantages for the synthesis of 1-D TiO₂ nanoparticles. First, the length and phase of the TiO₂ nanorods could be simultaneously controlled simply by varying the injection rate of the precursors. Second, the large-scale synthesis of uniform-sized nanorods could be achieved via the reaction of syringe pump delivered precursors. Third, the synthesized TiO₂ nanorods were successfully employed as the electrode materials for dye-sensitized solar cells.

Acknowledgment. We would like to thank the National Creative Research Initiative Program of the Korean Ministry of Science and Technology for the financial support.

Supporting Information Available: TEM image and XRD result of polydispersed TiO₂ nanoparticles synthesized by a short injection without using syringe pump; TEM images of TiO₂ nanorods taken at various reaction time intervals in the sampling experiments; XPS spectrum of TiO₂ nanorods before water treatment and after water treatment. This material is available free of charge via the Internet at <http://pubs.acs.org>.

References and Notes

- (1) (a) Xia, Y.; Yang, P.; Sun, Y.; Wu, Y.; Mayers, B.; Gates, B.; Yin, Y.; Kim, F.; Yan, H. *Adv. Mater.* **2003**, *15*, 353. (b) Jun, Y.-w.; Choi, J.-s.; Cheon, J. *Angew. Chem., Int. Ed.* **2006**, *45*, 3414. (c) Zhang, Z.; Sun, X.; Dresselhaus, M. S.; Ying, J. Y. *Phys. Rev. B* **2000**, *61*, 4850. (d) Yanson, A. I.; Bollinger, G. R.; van den Brom, H. E.; Agrait, N.; van Ruitenbeek, J. M. *Nature (London)* **1998**, *395*, 783. (e) Wang, Y.; Duan, X.; Cui, Y.; Lieber, C. M. *Nano Lett.* **2002**, *2*, 101. (f) Cui, Y.; Lieber, C. M. *Science* **2001**, *291*, 851. (g) Kovtyukhova, N. I.; Martin, B. R.; Mbindyo, J. K. N.; Smith, P. A.; Razavi, B.; Mayer, T. S.; Mallouk, T. E. *J. Phys. Chem. B* **2001**, *105*, 8762. (h) Huang, Y.; Duan, X.; Wei, Q.; Lieber, C. M. *Science* **2001**, *291*, 630. (i) Jun, Y.-w.; Lee, J.-H.; Choi, J.-s.; Cheon, J. *J. Phys. Chem. B* **2005**, *109*, 14795.
- (2) (a) Park, S.-J.; Kim, S.; Lee, S.; Khim, Z. G.; Chark, K.; Hyeon, T. *J. Am. Chem. Soc.* **2000**, *122*, 8581. (b) Dumestre, F.; Chaudret, B.; Amiens, C.; Respaud, M.; Fejes, P.; Renaud, P.; Zurcher, P. *Angew. Chem., Int. Ed.* **2003**, *42*, 5213. (c) Cordente, N.; Respaud, M.; Senocq, F.; Casanove, M. J.; Amiens, C.; Chaudret, B. *Nano Lett.* **2001**, *1*, 565.
- (3) (a) Holmes, J. D.; Johnston, K. P.; Doty, R. C.; Korgel, B. A. *Science* **2000**, *287*, 1471. (b) Wang, J. F.; Gudiksen, M. S.; Duan, X. F.; Cui, Y.; Lieber, C. M. *Science* **2001**, *293*, 1455. (c) Huynh, W. U.; Dittmer, J. J.; Alivisatos, A. P. *Science* **2002**, *295*, 2425. (d) Hu, J. T.; Li, L. S.; Yang, W. D.; Manna, L.; Wang, L. W.; Alivisatos, A. P. *Science* **2001**, *292*, 2060. (e) Hu, J.; Odom, T. W.; Lieber, C. M. *Acc. Chem. Res.* **1999**, *32*, 435. (f) Lieber, C. M. *Solid State Commun.* **1998**, *107*, 607-616. (g) Alivisatos, A. P. *Science* **1996**, *271*, 933. (h) Alivisatos, A. P. *J. Phys. Chem.* **1996**, *100*, 13226. (i) Yu, H.; Li, J.; Loomis, R. A.; Wang, L.-W.; Buhro, W. E. *Nat. Mater.* **2003**, *2*, 517. (j) Yu, H.; Li, J.; Loomis, R. A.; Gibbons, P. C.; Wang, L. W.; Buhro, W. E. *J. Am. Chem. Soc.* **2003**, *125*, 16168.
- (4) (a) Huang, M.; Mao, S.; Feick, H.; Yan, H.; Wu, Y.; Kind, H.; Weber, E.; Russo, R.; Yang, P. *Science* **2001**, *292*, 1897. (b) Johnson, J. C.; Choi, H. J.; Knutsen, K. P.; Schaller, R. D.; Saykally, R. J.; Yang, P.

- Nat. Mater.* **2002**, *1*, 101. (c) Johnson, J. C.; Yan, H.; Schaller, R. D.; Haber, L.; Saykally, R. J.; Yang, P. *J. Phys. Chem. B* **2001**, *105*, 11 387. (d) Dickson, R. M.; Lyon, L. A. *J. Phys. Chem. B* **2000**, *104*, 6095. (e) Johnson, J. C.; Yan, H.; Schaller, R. D.; Peterson, P. B.; Yang, P.; Saykally, R. J. *Nano Lett.* **2002**, *2*, 279. (f) Kind, H.; Yan, H.; Law, M.; Messer, B.; Yang, P. *Adv. Mater.* **2002**, *14*, 158. (g) Favier, F.; Walter, E. C.; Zach, M. P.; Benter, T.; Penner, R. M. *Science* **2001**, *293*, 2227. (h) Cui, Y.; Wei, Q.; Park, H.; Lieber, C. M. *Science* **2001**, *293*, 1289. (i) Law, M.; Kind, H.; Kim, F.; Messer, B.; Yang, P. *Angew. Chem., Int. Ed.* **2002**, *41*, 2405. (j) Colvin, V. L.; Schlamp, M. C.; Alivisatos, A. P. *Nature* **1994**, *370*, 354. (k) Kazes, M.; Lewis, D. Y.; Ebenstein, Y.; Mokari, T.; Banin, U. *Adv. Mater.* **2002**, *14*, 4, 317.
- (5) (a) Puentes, V. F.; Krishnan, K. M.; Alivisatos, A. P. *Science* **2001**, *291*, 2115. (b) Puentes, V. F.; Zanchet, D.; Erdonmez, C. K.; Alivisatos, A. P. *J. Am. Chem. Soc.* **2002**, *124*, 12 874. (c) Dumestre, F.; Chaudret, B.; Amiens, C.; Fromen, M.-C.; Casanove, M.-J.; Respaud, M.; Zurcher, P. *Angew. Chem., Int. Ed.* **2002**, *41*, 4286. (d) Qian, C.; Kim, F.; Ma, L.; Tsui, F.; Yang, P.; Liu, J. *J. Am. Chem. Soc.* **2004**, *126*, 1195.
- (6) (a) Murphy, C. J.; Jana, N. R. *Adv. Mater.* **2002**, *14*, 80. (b) Jana, N. R.; Gearheart, L.; Murphy, C. J. *J. Phys. Chem. B* **2001**, *105*, 4065. (c) Busbee, B. D.; Obare, S. O.; Murphy, C. J. *Adv. Mater.* **2003**, *15*, 414. (d) Xiong, Y.; Xie, Y.; Wu, C.; Yang, J.; Li, Z.; Xu, F. *Adv. Mater.* **2003**, *15*, 405. (e) Wu, H.-Y.; Chu, H.-C.; Kuo, T.-J.; Kuo, C.-L.; Huang, M. H. *Chem. Mater.* **2005**, *17*, 6447.
- (7) (a) Hanrath, T. T.; Korgel, B. A. *J. Am. Chem. Soc.* **2001**, *124*, 1424. (b) Lu, X.; Hanrath, T. T.; Johnston, K. P.; Korgel, B. A. *Nano Lett.* **2003**, *3*, 93. (c) Peng, X.; Manna, L.; Yang, W.; Wickham, J.; Scher, E.; Kadavanich, A.; Alivisatos, A. P. *Nature* **2000**, *404*, 59. (d) Pacholski, C.; Kornowski, A.; Weller, H. *Angew. Chem., Int. Ed.* **2002**, *41*, 1188. (e) Joo, J.; Na, H. B.; Yu, T.; Yu, J. H.; Kim, Y. W.; Wu, F.; Zhang, J. Z.; Hyeon, T. *J. Am. Chem. Soc.* **2003**, *125*, 11100. (f) Yu, J. H.; Joo, J.; Park, H. M.; Baik, S.-I.; Kim, Y. W.; Kim, S. C.; Hyeon, T. *J. Am. Chem. Soc.* **2005**, *127*, 5662. (g) Peng, Z. A.; Peng, X. G. *J. Am. Chem. Soc.* **2001**, *123*, 183. (h) Tang, Z.; Kotov, N. A.; Giersig, M. *Science* **2002**, *297*, 237. (i) Kan, S.; Mokari, T.; Rothenberg, E.; Banin, U. *Nat. Mater.* **2003**, *2*, 155.
- (8) (a) O'Regan, B.; Grätzel, M. *Nature* **1991**, *353*, 737. (b) Hagfeldt, A.; Grätzel, M. *Chem. Rev.* **1995**, *95*, 49. (c) Yan, S. G.; Prieskorn, J. S.; Kim, Y. J.; Hupp, J. T. *J. Phys. Chem. B* **2000**, *104*, 10871. (d) Lemon, B. I.; Hupp, J. T. *J. Phys. Chem. B* **1999**, *103*, 3797. (e) Kamat, P. V. *Chem. Rev.* **1993**, *93*, 267. (f) Stergiopoulos, T.; Arabatzis, I. M.; Katsaros, G.; Falaras, P. *Nano Lett.* **2002**, *2*, 1259.
- (9) (a) Kamat, P. V. *J. Phys. Chem. B* **2002**, *106*, 7729. (b) Subramanian, V.; Wolf, E.; Kamat, P. V. *J. Phys. Chem. B* **2001**, *105*, 11439. (c) Cho, Y.; Choi, W.; Lee, C.-H.; Hyeon, T.; Lee, H.-I. *Environ. Sci. Technol.* **2001**, *35*, 2988. (d) Tang, J.; Wu, Y.; McFarland, E. W.; Stucky, G. D. *Chem. Commun.* **2004**, 1670. (e) Han, S.; Choi, S.-H.; Kim, S.-S.; Cho, M.; Jang, B.; Kim, D.-Y.; Yoon, J.; Hyeon, T. *Small* **2005**, *1*, 812.
- (10) Iuchi, K.; Ohko, Y.; Tatsuma, T.; Fujishima, A. *Chem. Mater.* **2004**, *16*, 1165.
- (11) Cozzoli, P. D.; Kornowski, A.; Weller, H. *J. Am. Chem. Soc.* **2003**, *125*, 14539.
- (12) (a) Gao, X.; Zhu, H.; Pan, G.; Ye, S.; Lan, Y.; Wu, F.; Song, D. *J. Phys. Chem. B* **2004**, *108*, 2868. (b) Chen, Q.; Zhou, W.; Du, G.; Peng, L. M. *Adv. Mater.* **2002**, *14*, 1208. (c) Andersson, M.; Osterlund, L.; Ljungstrom, S.; Palmqvist, A. *J. Phys. Chem. B* **2002**, *106*, 10674. (d) Cheng, H.; Ma, J.; Zhao, Z.; Qi, L. *Chem. Mater.* **1995**, *7*, 6663. (e) Lou, X. W.; Zeng, H. C. *Chem. Mater.* **2002**, *14*, 4781. (f) Gui, Z.; Fan, R.; Mo, W.; Chen, X.; Yang, L.; Zhang, S.; Hu, Y.; Wang, Z.; Fan, W. *Chem. Mater.* **2002**, *14*, 5053. (g) Zhang, Q.; Gao, L. *Langmuir* **2003**, *19*, 967. (h) Yin, Q.; Wada, Y.; Kitamura, T.; Kambe, S.; Murasawa, S.; Mori, H.; Sakata, T.; Yanagida, S. *J. Mater. Chem.* **2001**, *11*, 1694. (i) Yanqing, Z.; Erwei, S.; Zhizhan, C.; Wenjun, L.; Xingfang, H. *J. Mater. Chem.* **2001**, *11*, 1547. (j) Li, Y.; Sui, M.; Ding, Y.; Zhang, G.; Zhuang, J.; Wang, C. *Adv. Mater.* **2000**, *12*, 818.
- (13) (a) Chemseddine, A.; Moritz, T. *Eur. J. Inorg. Chem.* **1999**, 235. (b) Lakshami, B. B.; Dorhout, P. K.; Martin, C. R. *Chem. Mater.* **1997**, *9*, 857. (c) Kasuga, T.; Hiramatsu, M.; Hoson, A.; Sekino, Niihara, K. *Adv. Mater.* **1999**, *11*, 1307. (d) Limmer, S. J.; Seraji, S.; Forbess, M. J.; Wu, Y.; Chou, T. P.; Nguyen, C.; Cao, G. *Adv. Mater.* **2001**, *16*, 1269. (e) Matsui, K.; Kyotani, T.; Tomita, A. *Adv. Mater.* **2002**, *14*, 1216. (f) Wang, W.; Gu, B.; Liang, L.; Hamilton, W. A.; Wesolowski, D. J. *J. Phys. Chem. B* **2004**, *108*, 14789. (g) Li, Y.; Fan, Y.; Chen, Y. *J. Mater. Chem.* **2002**, *12*, 1387. (h) Martin, C. R. *Science* **1994**, *266*, 1961. (i) Miao, Z.; Xu, D.; Ouyang, J.; Guo, G.; Zhao, X.; Tang, Y. *Nano Lett.* **2002**, *2*, 7, 717.
- (14) (a) Jun, Y.; Casula, M. F.; Sim, J.; Kim, S. Y.; Cheon, J.; Alivisatos, A. P. *J. Am. Chem. Soc.* **2003**, *125*, 15981. (b) Adachi, M.; Murata, Y.; Takao, J.; Jiu, J.; Sakamoto, M.; Wang, F. *J. Am. Chem. Soc.* **2004**, *126*, 14943. (c) Muhr, H. J.; Krumeich, F.; Schonholzer, U. P.; Bieri, F.; Niederberger, M.; Gauckler, L. J.; Nesper, R. *Adv. Mater.* **2000**, *12*, 231. (d) Yada, M.; Mihara, M.; Mouri, M.; Kuroki, M.; Kijima, T. *Adv. Mater.* **2002**, *14*, 309. (e) Wang, C.; Deng, Z.; Li, Y. *Inorg. Chem.* **2001**, *40*, 5210. (f) Yang, P.; Zhao, D.; Margolese, D. I.; Chmelka, B. F.; Stucky, G. D. *Chem. Mater.* **1999**, *11*, 2813. (g) Jiang, X.; Wang, Y.; Herricks, T.; Xia, Y. *J. Mater. Chem.* **2004**, *14*, 695. (h) Seo, J.-W.; Jun, Y.-W.; Ko, S. J.; Cheon, J. *J. Phys. Chem. B* **2005**, *109*, 5389.
- (15) (a) Hosono, E.; Fujihara, S.; Kakiuchi, K.; Imai, H. *J. Am. Chem. Soc.* **2004**, *126*, 7790. (b) Macak, J. M.; Tsuchiya, H.; Schmuki, P. *Angew. Chem., Int. Ed.* **2005**, *44*, 2. (c) Imai, H.; Matsuta, M.; Shimizu, K.; Hirashima, H.; Negishi, N. *J. Mater. Chem.* **2000**, *10*, 2005. (d) Hulteen, J. C.; Martin, C. R. *J. Mater. Chem.* **1997**, *7*, 1075. (e) Peng, X.; Chen, A. *J. Mater. Chem.* **2004**, *14*, 2542. (f) Wu, J.; Yu, C. *J. Phys. Chem. B* **2004**, *108*, 3377. (g) Park, I.; Jang, S.; Hong, J. S.; Vittal, R.; Kim, K. *Chem. Mater.* **2003**, *15*, 4633.
- (16) (a) Vioux, A. *Chem. Mater.* **1997**, *9*, 2292. (b) Arnal, P.; Corriu, R. J. P.; Leclercq, D.; Mutin, P. H.; Vioux, A. *Chem. Mater.* **1997**, *9*, 694. (c) Trentler, T. J.; Denler, T. E.; Bertone, J. F.; Agrwal, A.; Colvin, V. L. *J. Am. Chem. Soc.* **1999**, *121*, 1613. (d) Niederberger, M.; Bartl, M. H.; Stucky, G. *Chem. Mater.* **2002**, *14*, 4364. (e) Niederberger, M.; Bartl, M. H.; Stucky, G. D. *J. Am. Chem. Soc.* **2002**, *124*, 13642. (f) Joo, J.; Yu, T.; Kim, Y. W.; Park, H. M.; Wu, F.; Zhang, J. Z.; Hyeon, T. *J. Am. Chem. Soc.* **2003**, *125*, 6553. (g) Tang, J.; Fabbri, J.; Robinson, R. D.; Zhu, Y.; Herman, I. P.; Steigerwald, M. L.; Brus, L. E. *Chem. Mater.* **2004**, *16*, 1336.
- (17) (a) Joo, J.; Kwon, S. G.; Yu, T.; Cho, M.; Lee, J.; Yoon, J.; Hyeon, T. *J. Phys. Chem. B* **2005**, *109*, 15297. (b) Joo, J.; Kwon, S. G.; Yu, J. H.; Hyeon, T. *Adv. Mater.* **2005**, *17*, 1873.
- (18) (a) Park, J.; Koo, B.; Hwang, Y.; Bae, C.; An, K.; Park, J.-G.; Park, H. M.; Hyeon, T. *Angew. Chem., Int. Ed.* **2004**, *43*, 2282. (b) Park, J.; Koo, B.; Yoon, K. Y.; Hwang, Y.; Kang, M.; Park, J.-G.; Hyeon, T. *J. Am. Chem. Soc.* **2005**, *127*, 8433.
- (19) (a) Hurum, D. C.; Agrios, A. G.; Gray, K. A.; Rajh, T.; Thurnauer, M. C. *J. Phys. Chem. B* **2003**, *107*, 4545. (b) Hurum, D. C.; Gray, K. A.; Rajh, T.; Thurnauer, M. C. *J. Phys. Chem. B* **2005**, *109*, 977. (c) Wu, C.; Yue, Y.; Deng, X.; Hua, W.; Gao, Z. *Catal. Today* **2004**, *93*, 863.
- (20) Spurr, R. A.; Myers, H. *Anal. Chem.* **1957**, *29*, 760.
- (21) (a) Garvie, R. C. *J. Phys. Chem.* **1978**, *82*, 218. (b) Garvie, R. C. *J. Phys. Chem.* **1965**, *69*, 1238. (c) Zhang, H.; Banfield, J. F. *J. Mater. Chem.* **1998**, *8*, 2073. (d) Huang, F.; Banfield, J. F. *J. Am. Chem. Soc.* **2005**, *127*, 4523. (e) Hu, Y.; Tsai, H.-L.; Huang, C.-L. *Mater. Sci. Eng., A* **2003**, *344*, 209. (f) Ding, X.; Liu, X. *J. Alloys. Compd.* **1997**, *248*, 143. (g) Gibb, A. A.; Banfield, J. F. *Am. Mineral.* **1997**, *82*, 717.